Available online at www.sciencedirect.com

SCIENCE DIRECT®

Biochimica et Biophysica Acta 1655 (2004) 184–194

BIOCHIMICA ET BIOPHYSICA ACTA

BBA

www.bba-direct.com

Review

Time-resolved oxygen production by PSII: chasing chemical intermediates ☆

Jürgen Clausen[a], Richard J. Debus[b], Wolfgang Junge[a,*]

[a] *Abteilung Biophysik, Fachbereich Biologie/Chemie, Barbarastr. 11, Universität Osnabrück, D-49069 Osnabrück, Germany*

[b] *UCR Biochemistry, University of California at Riverside, Riverside, CA, USA*

Received 11 March 2003; received in revised form 25 June 2003; accepted 25 June 2003

Abstract

Photosystem II (PSII) produces dioxygen from water in a four-stepped process, which is driven by four quanta of light and catalysed by a Mn-cluster and tyrosine Z. Oxygen is liberated during one step, coined $S_3 \Rightarrow S_0$. Chemical intermediates on the way from reversibly bound water to dioxygen have not yet been tracked, however, a break in the Arrhenius plot of the oxygen-evolving step has been taken as evidence for its existence.

We scrutinised the temperature dependence of (i) UV-absorption transients attributable to the reduction of the Mn-cluster and tyrosine Z by water, and (ii) polarographic transients attributable to the release of dioxygen. Using a centrifugatable and kinetically competent Pt-electrode, we observed no deviation from a linear Arrhenius plot of oxygen release in the temperature range from −2 to 32 °C, and hence no evidence, by this approach, for a sufficiently long-lived chemical intermediate. The half-rise times of oxygen release differed between *Synechocystis* WT* (at 20 °C: 1.35 ms) and a point mutant (D1–D61N: 13.1 ms), and the activation energies differed between species (*Spinacia oleracea*, 30 kJ/mol versus *Synechocystis*, 41 kJ/mol) and preparations (PSII membranes, 41 kJ/mol versus core complexes, 33 kJ/mol, *Synechocystis*).

Correction for polarographic artefacts revealed, for the first time, a temperature-dependent lag-phase of the polarographic transient (duration at 20 °C: 0.45 ms, activation energy: 31 kJ/mol), which was indicative of a short-lived intermediate. It was, however, not apparent in the UV-transients. Thus the "intermediate" was probably newly formed and transiently bound oxygen.

Keywords: Photosynthesis; Water oxidation; Activation energy; S-state; Photosystem II

1. Introduction

Photosystem II (PSII) of green plants and cyanobacteria evolves oxygen after absorption of four quanta of light. Each step oxidises a chlorophyll *a* moiety, P_{680}, and transfers one electron via pheophytin to a bound quinone, Q_A. $Q_A^{\cdot -}$ reduces a second quinone, Q_B. $P_{680}^{\cdot +}$ is reduced by the secondary donor, Y_Z (Tyr161 on the D1 subunit of PSII) to yield Y_Z^{ox}, which is in turn reduced by the oxygen-evolving complex (OEC, i.e. the Mn-cluster plus ligands plus bound water). The OEC contains a tetranuclear manganese cluster. Sequential absorption of light cycles the OEC through a series of redox states, S_n, where n indicates the number of stored oxidising equivalents ($n = 0 \ldots 4$). S_4 spontaneously decays into S_0 resulting in the release of dioxygen from water. The dark stable resting state of the OEC is S_1, and as a result, oxygen evolution from dark-adapted samples peaks on the third flash and subsequently every fourth flash (for reviews, see Refs. [1–8]).

It is generally accepted that each of three successive steps leading from S_0 to S_3 places one oxidising equivalent on the Mn-cluster plus its ligands (for a recent account on Mn

Abbreviations: β-DM, *n*-dodecyl β-D-maltoside; chl, chlorophyll; D1, D2, core subunits of Photosystem II; ET, electron transfer; DCBQ, 2,5-dichlorobenzoquinone; DCMU, 3-(3′,4′-dichlorophenyl)-1,1′-dimethylurea; FWHM, full-width at half-maximum; MES, 2-(*N*-morpholino)-ethanesulfonic acid; OEC, oxygen-evolving complex; P_{680}, primary electron donor of PSII; PSII, Photosystem II; Q_A, Q_B, bound quinone acceptors in PSII; S_i, (i=0–4), redox states of the catalytic centre; Y_D, redox-active tyrosine-160 of D2 with auxiliary function; Y_Z, redox-active tyrosine-161 of D1

☆ This article is dedicated to the late Jerry Babcock, i.a. pioneer of time-resolved EPR of the catalytic centre of oxygen production by Photosystem II.

* Corresponding author. Tel.: +49-541-969-2872; fax: +49-541-969-2262.

E-mail address: junge@uos.de (W. Junge).

0005-2728/$ - see front matter © 2004 Elsevier B.V. All rights reserved.
doi:10.1016/j.bbabio.2003.06.001

versus ligand oxidation, see Ref. [9]). Bound water is rapidly exchangeable during all states up to S_3 [10–13]. The fourth step converts state S_3Y_Z into $S_3Y_Z^{ox}$, which decays into S_0 plus dioxygen. So far, $S_3Y_Z^{ox}$ has been the only sizeable intermediate between [S_3] and [S_0 plus dioxygen]; it is the only entity presently representing the intermediate that has been coined S_4 [14,15]. A peroxide has been postulated on the way from bound water to dioxygen [16]. Although incorporated in recent reaction schemes [8,17,18], it has so far escaped detection. Structural models of PSII at 0.37 [19] and 0.38 nm [20,21] don't provide mechanistic clues, yet.

It has been attempted to resolve the reaction $(H_2O)_2S_3Y_Z^{ox} \rightarrow S_0Y_Z^{red} + 4H^+ + O_2$ kinetically by (i) O_2-polarography [17,22–27], (ii) UV-absorption spectrophotometry [17,27–33], (iii) EPR-spectroscopy of $Y_{\dot{Z}}$ [34], (iv) EPR-oxymetry [35–37], and (v) by recording pH transients (see, e.g. Refs. [17,38]).

Circumstantial evidence for the existence of an intermediate has been inferred from a break in the Arrhenius plot of UV-absorption transients around 360 nm. Spectroscopic measurements at 355 nm with PSII core complexes of the thermophilic cyanobacterium *Synechococcus vulcanus* Copeland [31], showed a discontinuity of the activation energy (E_a), as evident from a kink (at $T = 16$ °C) in the Arrhenius plot. Later the same group reported a (weakly pronounced) kink at 6 °C for membrane fragments (BBY) from spinach [39] and another one at 11 °C for PSII core complexes from spinach [40]. On the basis of these kinks, Renger [8,41], Koike et al. [31], Renger and Hanssum [39], and Karge et al. [40] proposed that S_3 is a redox-isomeric state composed of two substates, S_3(I) and S_3(II), the latter with peroxide character (see also Ref. [18]). Performing similar UV experiments, and using PSII core complexes from *Pisum sativum*, however, we did not observe any break in the linear Arrhenius plot in the temperature region from 7.9 to 30.6 °C [17].

Another way to track down intermediates of oxygen evolution was the search for time lags in the final transition of water oxidation, $S_3Y_Z^{ox} \rightarrow S_0Y_Z$. Two groups have reported such lags in kinetic studies. The lag-phase as reported in this work was longer (450 μs at 20 °C) than those reported by other groups. Razeghifard and Pace [37] reported a lag shorter than 50 μs under similar conditions by EPR-oxymetry which became longer (200 μs) only at low pH or at high salt. Rappaport et al. [15] measured the reduction of Y_Z^{ox} at a wavelength of 295 nm and found a short lag phase with a half-time of 30 μs in $S_0Y_Z^{ox} \rightarrow S_1Y_Z$ and 50 μs in $S_3Y_Z^{ox} \rightarrow S_0Y_Z$. It was noteworthy that the lag phase reported in our work here *followed* the electron transfer reaction, whereas the ones of the former reports preceded it.

This discrepancy between experimental results, and the need to pin down any hint for an intermediate has prompted us to reinvestigate this matter. A repeat of the UV photometric experiment on the reaction $S_3Y_Z^{ox} \rightarrow S_0 + O_2$, again yielded a perfectly straight Arrhenius plot in the now extended temperature range down to 3.9 °C (see Fig. 6 in this article). Thus we focussed on a kinetic resolution of oxygen release. Oxygen production by photosynthesis has been polarographically recorded at high time resolution by bare Pt-electrodes. To overcome the diffusion limitation of oxygen transfer to the electrode surface, oxygen-evolving material has been layered on the surface. Sinclair and Arnason [42] used a dispersive method with sinoidal modulation of continuous light, whereas Lavorel [43] applied flashing light to dark-adapted material. Both groups analysed the diffusion problem theoretically and corrected the observed polarographic transients for the effects of diffusion limitation. These sophisticated approaches were still limited, mainly for two reasons: (i) the packing distribution in the first layer, has remained an uncontrolled parameter, and (ii) the original signals were not free of artefacts (see Fig. 5 in Ref. [43] some milliseconds after the flash of light). Thus we started with an analysis of the kinetic competence of a centrifugatable oxygen electrode to proceed to the question of linear versus kinked Arrhenius behaviour of oxygen production after a flash of light.

2. Materials and methods

Cells of the modified "wild-type" (WT*) [44] and of the mutant D1–D61N of *Synechocystis* sp. were cultivated as described by Ref. [45] but in an atmosphere enriched with 4% of CO_2 under illumination with (cool-white) fluorescent light at 0.8–1.4 mW cm^{-2}. The mutants were constructed in a strain of *Synechocystis* that lacks PSI and *apc*E function [46]. The medium was supplemented with 15 mM glucose. Cells were harvested by centrifugation at $OD_{740} = 0.9–1.1$, resuspended in buffer F (40 mM MES-NaOH pH 6.35, 10 mM $CaCl_2$, 10 mM $MgCl_2$ and 50% (v/v) glycerol) and stored at −80 °C. The concentration of chlorophyll *a* was 57–76 μM (determined according to Ref. [47]). The modified WT* is a strain of *Synechocystis* that lacks PSI and *apc*E function [46], and contains only one *psbA* gene.

Oxygen-evolving membranes from *Synechocystis* WT* cells were prepared following Ref. [48] with some minor modifications. Cells were broken with glass beads with a diameter of 500 μM instead of 100 μM. The membrane fragments were pelleted by centrifugation at 150,000 × *g* for 30 min. After the final resuspension the chl-concentration was measured and the membranes were frozen in liquid nitrogen and stored at −80 °C. Membrane fragments from spinach (BBY) were prepared as described in Ref. [49] with modifications described in Ref. [50].

Flash-induced release of O_2 was measured polarographically with a bare platinum electrode. Oxygen-evolving membranes were suspended at 2.7–5.4 μM (*Synechocystis* membranes) or 10 μM (spinach BBY) chlorophyll in buffer HMCS-HSB1 (50 mM Hepes pH

7.2, 200 mM NaCl, and 5 mM $CaCl_2$, 10 mM $MgCl_2$, 1 M sucrose, 1 M glycine betaine). To increase the time resolution, aliquots of 30 μl were deposited on the electrode, and the membranes were pelleted upon the platinum electrode by centrifugation (1700 × *g*, 10 min, 14 °C, Beckmann TJ6 centrifuge, swing-out rotor) in complete darkness. The cathode (Pt) was negatively polarised with −800 mV against the anode (Ag/AgCl) and connected to a current-to-voltage amplifier (home-built). When a voltage step was applied directly to the amplifier, the half-rise time was about 100 μs). The polarization voltage of −800 mV was applied to the Pt-electrode 1 min before the measurements started. Polarographic transients were digitised and recorded by a Nicolet Pro30 recorder.

2.1. Kinetic measurements

After pelleting of the sample, the electrode block was thermally equilibrated for 20 min in contact with a thermostated bath (Julabo F31-C). During equilibration the sample was kept in total darkness. A single train of three flashes (Xenon-flash lamp, filter, Schott RG610, pulse width: full-width at half-maximum (FWHM) 10 μs, 1 s between flashes) was applied to the fresh sample. The temperature was monitored in the sample with a GTH 175/molybdenum element. The analogue rise time, limited by electrode/amplifier, was ($t_{1/2}$ = 100 μs), as mentioned, and the digital address time of the averager was set at 20 μs.

2.2. Oxygen pattern

Two trains of 15 flashes at intervals of 1 s were recorded at room temperature, and at lower time resolution (500 μs/address). Only the transients from the second train (recorded after another 10 min of dark adaptation) were used and fitted with three Kok parameters (percentage of misses (α), double hits (β) and the distribution of S-states after dark-adaption (%S_1)) according to Ref. [51]. The flash-dependent oxygen yield was taken from the maximal extent per flash, not from the area beneath the curve, as previously [24]. The probability for α and β was kept constant for all S-states.

For flash-spectrophotometric measurements [52], PSII core particles were suspended in 50 mM MES pH 6.6, 1 M sucrose, 25 mM $CaCl_2$, 10 mM NaCl, 1 M glycine betaine, 0.06% *n*-dodecyl β-D-maltoside (β-DM w/v); 200 μM DCBQ (2,5-dichloro-*p*-benzoquinone) was used as electron acceptor. Electron transfer from the Mn-cluster to Y_Z^{ox} was recorded at a wavelength of 360 nm under excitation with five saturating flashes (100 ms between flashes). We used repetitively dark-adapted core particles (8–12 μM chl, 2 min dark adaptation) as detailed elsewhere [53]. The samples were excited by a Nd:YAG laser (532 nm, FWHM 6 ns). The optical pathlength was 1 cm. The time resolution was 50 μs/address. Transients were digitised and recorded by a Nicolet Pro30 recorder. Spectroscopic data were fitted by standard routines of the program Origin (Microcal).

3. Results

3.1. Polarographic-transients at high time resolution and their correction

The oxygen evolution of membranes from the unicellular cyanobacterium *Synechocystis* sp. PCC6803 was measured as a function of the ambient temperature using a centrifugatable, bare platinum electrode. Dark-adaptation and thermostating for 20 min at room temperature affected neither the extent nor the rate of the polarographic transient as compared with the one obtained right after centrifugation. Even higher sample stability was expected at lower temperatures. Core complexes could be stored at room temperature in the dark for over 1 h without any decrease of the activity.

With oxygen-evolving membranes from *Synechocystis*, the pattern of oxygen evolution in trains of 15 flashes compared well with data from the literature [22,23]. We determined the following Kok-parameters (after 10 min of dark adaptation): 12.3% misses (α), 3.2% double-hits (β) and a distribution over the S-states ($S_0/S_1/S_2/S_3$) of 20.4/79.6/0/0. Fig. 1 shows data points (squares) and the fit (straight line) based on this parameter set.

Raw data of a typical polarographic transient upon the third flash in a row are displayed in Fig. 2A. The transient revealed three characteristic regions: (i) the flash artefact, (ii) the rise of the polarographic current due to the pulsed oxygen production, and (iii) the consumption of oxygen by the electrode.

(i) The flash artefact was observed even without a sample on the electrode. It was composed of (1) a negative transient

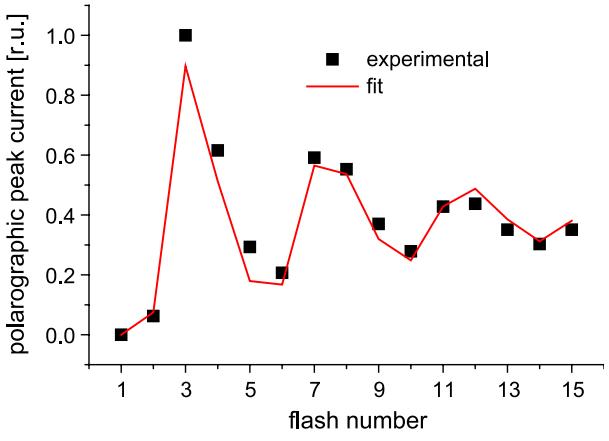

Fig. 1. Pattern of oxygen release in PSII membranes from *Synechocystis*. The amplitude of the polarographic signal as a function of the flash number. Data were fitted with the following Kok-parameters: α = 12.3%, β = 3.2% and the initial dark distribution $S_0/S_1/S_2/S_3$ = 20.4/27.6/0/0. Solid line = calculated; squares = experimental (For color see online version).

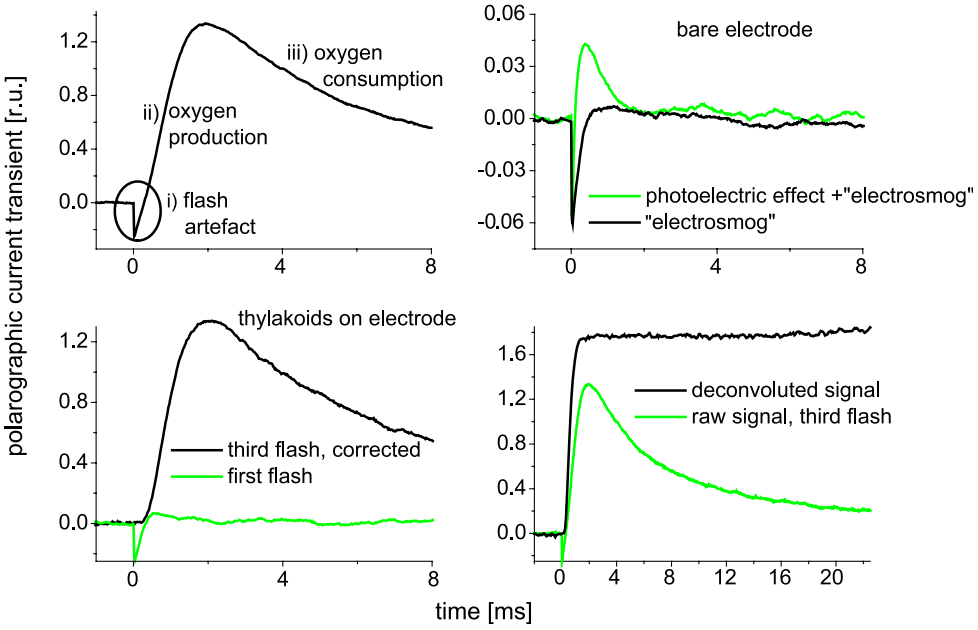

Fig. 2. Polarographic transients, raw and corrected data. (A) Raw signal with three characteristic features: (i) the flash artefact, partly superimposed by (ii) the rising polarographic signal (=oxygen production). (iii) Decay=oxygen consumption by the electrode. (B) Flash-induced artefacts of the electrode. Electrosmog (dark line) and superimposition (bright line) of photoelectric effect (see text) and electrosmog. The electrosmog, alone, was apparent when the light guide was not connected to the electrode. Both curves were recorded without any biological sample (only buffer) on the electrode. Ten measurements averaged. (C) Bright line: artefact after the first flash. Dark line: polarographic transient (third flash, 5.43 μM Chl, 28.7 °C) after subtraction of the flash-artefact of the first flash. (D) Polarographic signal after the third flash (bright line, single measurement). Artefact and decay are clearly visible, 5.43 μM chl, 28.7 °C. The dark line represents the same trace after subtraction of the artefacts and after deconvolution of the decay with two exponentials. Half-rise time=0.65 ms. Time resolution=20 μs/point (For color see online version).

(see Fig. 2B, dark) that was attributable to "electrosmog", it was observed even after optical shielding of the flash lamp, and (2) a positive transient, the photoelectric flash artefact [54]. This positive "bulge" was only observed if the light guide was connected to the electrode. The bright transient in Fig. 2B represents the superimposition of both types of artefacts. The photoelectric flash-artefact was virtually temperature-independent, its rise time was the same as found when applying an external voltage-jump to the amplifier (100 μs). It was noteworthy that there was no temperature-dependence of the instrumental time resolution. Moreover, the flash artefact was independent of the flash number in a train. Identical artefacts were observed on the first and second flash with a 3-(3′,4′-dichlorophenyl)-1,1′-dimethylurea (DCMU)-inhibited sample (data not shown).

To approximate the illumination conditions of any particular sample that was layered on to the electrode, the artefact was recorded as the transient upon the first flash in a series, which according to the data shown in Fig. 1 (and according to the dark equilibrium between the S-states) did not produce oxygen. Fig. 2C shows the artefact (in grey) and the corrected polarographic transient (in black). A striking feature of the oxygen transient after correction was the clear disclosure of the *lag phase* (see below).

(iii) The decay of the polarographic signal was owed to the consumption of oxygen by the electrode and to diffusion of oxygen away from the electrode. The polarographic transient was deconvoluted with two exponential functions to reveal the (consumption-free) current owed oxygen production (dark transient in Fig. 2D). The corrected extent of oxygen evolution was greater than the one of the raw transient.

(ii) The rise of the polarographic transient occurred in the time domain of 1 ms in the wild-type and of more than 10 ms in a particular mutant. It was a function of the velocity of the production of dioxygen, its release from the catalytic centre and the diffusion to and the reaction with the electrode. The intrinsic response time of the electrode/amplifier, 100 μs, thus was not limiting. The diffusion time depends on the distance between the source of oxygen and the electrode (see, e.g. Ref. [43]), and thereby on the layering of material on its surface. We screened the dependence on the chlorophyll concentration before centrifugation of (a) the half-rise time ($\tau_{1/2}$), (b) the duration of the lag phase (t_{lag}), and (c) the extent of the polarographic signal. Fig. 3 shows raw polarographic transients at two chlorophyll concentrations, 5.4 and 54 μM, displayed at wide (Fig. 3A) and narrow time spread (Fig. 3B). Broadly speaking, neither the rise time nor the lag phase were affected, whereas the decay was. The latter was expected because a thicker layer represented a greater oxygen capacity and a longer relaxation time of the oxygen pulse. We analysed 11 deconvoluted polarographic transients (see Fig. 2D, dark transient for a deconvoluted signal) that were recorded at

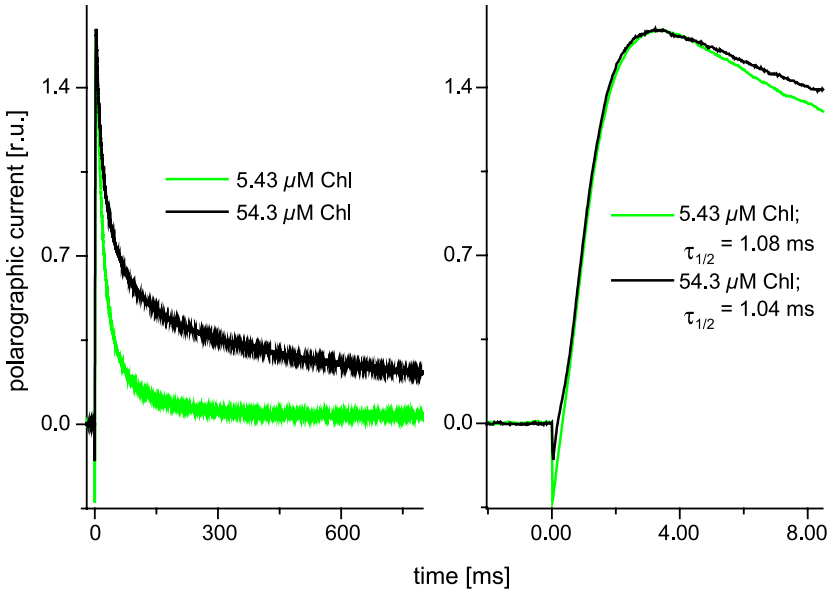

Fig. 3. Polarographic transients under variation of the amount of material deposited on the electrode by centrifugation. Time resolution = 20 μs/point, extent normalised. Dark line = 54.3 μM Chl, bright line = 5.43 μM chl. (A) Wide time spread; the decay was significantly slowed down by higher concentration of material during centrifugation. (B) Narrow time spread; both the time lag and the rise were unaffected by the tenfold increase of centrifuged material (For color see online version).

chlorophyll concentrations ranging from 1.4 to 33 μM at a temperature of 17.6 °C. The mean values (and standard deviations) were as follows: the half-rise time $t_{1/2}$ = 1.02 ms (11%) and the lag-time t_{lag} = 0.44 ms (14%). The amount of layered material was without significant influence on the rate of oxygen evolution. However, as expected, it severely affected the decay time of the flash-induced oxygen step by consumption at the electrode (see Fig. 3). Even when using the same concentration of chlorophyll in a series of seemingly identical experiments with the same batch of starting materials, the decay time of the polarographic transients varied from sample to sample, i.e. from centrifugation to centrifugation run, whereas the rise and lag time did not.

At this point, it was noteworthy that different packing of the material on the electrode neither affected the lag nor the rise of the corrected polarographic signal.

Lavorel's [43] theoretical analysis of the diffusion controlled transmission to the electrode of an infinitely sharp oxygen step from a thin layer of sources at fixed distance X predicts a time lag whose duration is proportional to the rise- and the decay-time of the polarographic transient. We checked the origin of the time lag, whether it was caused by (i) the diffusion-controlled oxygen transmission to the electrode or by (ii) the oxygen liberation from the layered source. Oxygen transients were recorded using PSII membranes from a mutant, *Synechocystis* D61N (data shown in Fig. 4). At room-temperature (≈ 20 °C) the half-rise time was 13.1 ms, i.e. more than 10 times longer than in WT*, but the duration of the time lag in the mutant remained the same as in WT* (0.4 ms in D61N and 0.45 ms in WT*). At 2.7 °C the rise time in WT* was 3.2 ms and the lag time increased to 1 ms. That the prolongation of the rise time in the mutant was attributable to the electron transfer itself, and not to some alteration of the diffusive supply of O_2 to the electrode, was evident from a comparison of the flash-induced UV absorption transients. They were likewise slowed down in the mutant (1.22 ms WT*, ca. 13.7 ms D61N; data not shown).

In conclusion, the time lag of the polarographic transient was not owed to the diffusion-controlled transmission of oxygen from the source to the electrode, but probably to the release of preformed, but bound/adsorbed oxygen from the protein into the medium.

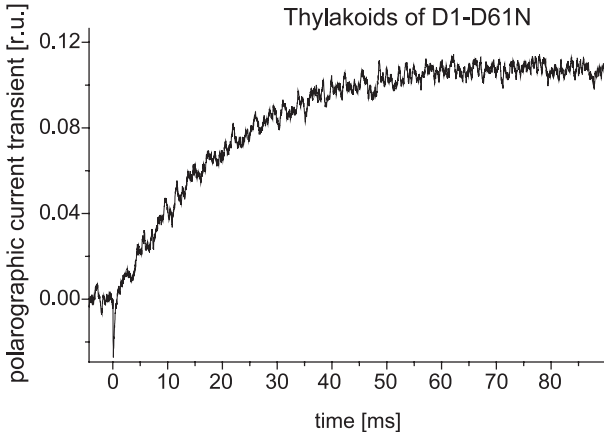

Fig. 4. Raw polarographic transient recorded with PSII membranes from the point mutant D1–D61N. Time resolution = 20 μs/point. Five recordings averaged, 30 μM Chl applied to the electrode. The half-rise time was 13.1 ms and the duration of the lag-phase was 0.4 ms.

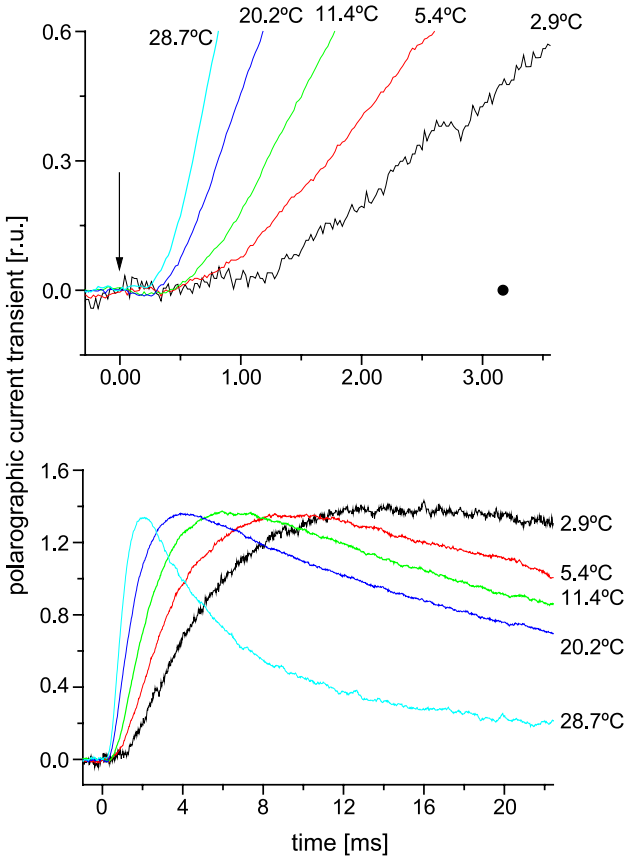

Fig. 5. The lag-phase of polarographic transients upon the third flash in a series under variation of the temperature. Dark-adapted PSII membranes of *Synechystis* sp. PCC6803 (centrifuged on a bare platinum electrode). (A) Narrow time spread. Temperatures and durations of the lag were as follows: 28.7 °C (0.32 ms), 20.2 °C (0.45 ms), 11.4 °C (0.63 ms), 5.4 °C (0.91 ms) and 2.9 °C (0.94 ms). [Chl] = 5.43 μM, time resolution = 20 μs/point. The transients were normalised and flash artefacts subtracted (see text and Fig. 2). The expected duration of a diffusion-limited lag-phase according to Lavorel [43] ($t_{lag} = 0.218 \times t_M$) is represented by the black dot applying to a temperature of 2.9 °C. The arrow indicates the flash. For t_M (time of maximum) see panel B. (B) Same data as in panel A, but with a wide time spread. The extent was normalised, the flash artefact subtracted (see Fig. 2), but the decay was not corrected by deconvolution. Temperatures and half-rise times (after deconvoluting the signals) were as follows: 28.7 °C (0.65 ms), 20.2 °C (1.01 ms), 11.4 °C (1.58 ms), 5.4 °C (2.29 ms), 2.9 °C (3.7 ms) (For color see online version).

3.2. Arrhenius plots of the lag and rise of polarographic transients attributable to oxygen evolution

The temperature dependence of the lag and the rise of polarographic transients on the third flash in a row was determined in the range from −2.1 to 31.7 °C. The lag-times and the half-rise times were determined after deconvolution for a total of 75 samples of oxygen-evolving membranes of *Synechocystis* sp. PCC6803. Examples of artefact-corrected data are given in Fig. 5. The transients are shown without deconvolution to reveal the temperature effect on the oxygen consumption by the electrode. The rise times, which are discussed in the following, however, were determined after deconvolution. The rates of the rise were determined for each sample, averaged for each temperature (typ. $n = 3$) and inserted into an Arrhenius plot (see dark points in Fig. 6). Over the temperature range from −2.1 to 31.7 °C the points laid on a straight line yielding an activation energy of $E_a = 40.75$ (±0.9) kJ/mol and a preexponential factor, A, with a log-value of ln $A = 16.3$ (±0.4). There was no evidence for any break-point. At 20 °C the line of best fit yielded a half-rise time for oxygen evolution of 1.1 ms. The lag-time increased with decreasing temperatures (see Fig. 5). The activation energy of the lag-phase was 31.1 (±0.9) kJ/mol (data not shown).

We repeated this series of experiments with BBY membranes from spinach in the temperature range from 0.82 to 30.8 °C. The Arrhenius plot (not shown) was again perfectly linear but revealed a different activation energy of $E_a = 29.8 \pm 0.8$ kJ/mol and a preexponential factor ln $A = 15.9 \pm 0.3$. Signal amplitudes (data not shown) were much smaller than with *Synechocystis* membranes. In conclusion: the Arrhenius analysis of oxygen evolution gave no evidence for a temperature-dependent switching from one particular to another rate-limiting reaction.

Also represented in Fig. 6 (open circles) is the expected Arrhenius plot of a diffusion controlled reaction, whose

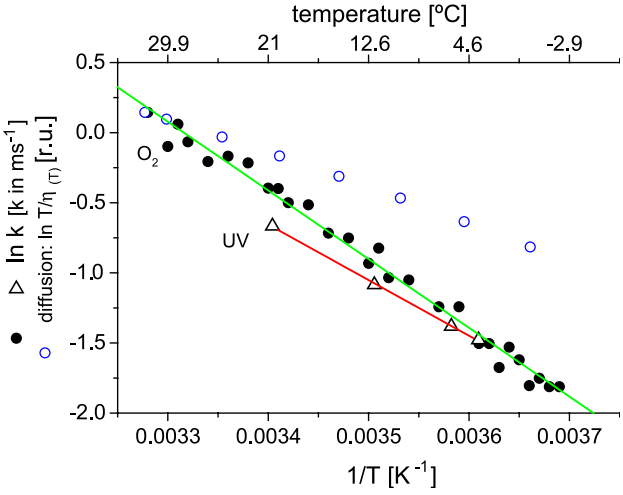

Fig. 6. Arrhenius plot of the $S_3 \Rightarrow S_4 \rightarrow S_0$ transition. Solid circles: the rate of oxygen evolution as determined from corrected polarographic transients with PSII membranes (5.43 μM chl) from *Synechocystis* species (see Fig. 5). The linear fit resulted in an E_a of 40.75 kJ/mol (±0.9); ln $A = 16.3$ (±0.4). Triangles: the rate of UV-transients at 360 nm with PSII core complexes of *Synechocystis* species (see Fig. 7). E_a was 33 (±1) kJ/mol; ln $A = 12.8$ (±0.2). Open circles: the "expected Arrhenius plot" of oxygen-diffusion in water. It showed a low apparent E_a of 20.7 kJ/mol. For 20 °C the line of best fit yielded a half-rise time for oxygen evolution of 1.1 ms. This was in good agreement with data from the literature, ranging from 1 to 1.5 ms, as obtained by different methods [15,17,22,23,26,28–33,59,60]. The half-rise times were longer than the values determined by time-resolved EPR-oximetry with spinach thylakoids (0.4 [35] and 0.75–0.85 ms at 8–10 °C [36,37]). It is worth recalling that the first time-resolved measurements by EPR of the reduction of tyrosine Z was performed by Gerald T. Babcock et al. [34] (For color see online version).

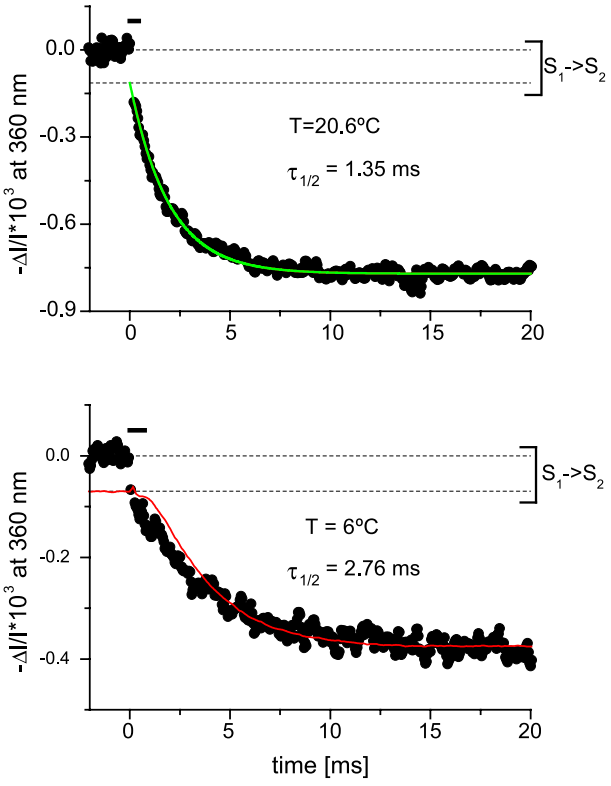

Fig. 7. Absorption transients at 360 nm during the $S_3 \Rightarrow S_4 \rightarrow S_0$ transition in dependence of the temperature. Core complexes of *Synechocystis* species. Difference of third minus fifth flash (see text). The dashed lines indicate the unresolved jump due to the $S_1 \Rightarrow S_2$ transition (see text). (A) 20.6 °C, half-rise time = 1.35 ms, 70 transients averaged. (B) 6 °C, half-rise time = 2.76 ms, 85 transients averaged. Data were smoothed over every second point. 8–12 μm Chl, 200 μM DCBQ. The solid vertical bar represents the expected duration of the lag-phase as inferred from polarographic measurements (see also the bright line) at 5.5 °C (For color see online version).

temperature dependence is governed by the viscosity of water (see Ref. [55]). This yielded an apparent activation energy of only 20.7 kJ/mol, about one-half of the one which we observed for oxygen evolution (40.8 kJ/mol). Fig. 6 also shows an Arrhenius plot of UV-transients (see following section).

3.3. Arrhenius plot of the UV-transients at 360 nm which are indicative of the electron transfer into and between the Mn-cluster to Y_Z

In the foregoing, we used PSII *membranes* for layering oxygen-evolving material on the electrode by centrifugation. The spectroscopic measurements in the UV, on the other hand, were carried out with less scattering PSII core complexes which provide much better signal-to-noise ratio. PSII core complexes of *Synechocystis* were dark-adapted, then excited with a series of short laser flashes, and absorption transients were recorded at a wavelength of 360 nm at different temperatures. Each of the transients which are shown in Fig. 7 represents the difference between the raw transients that were observed upon the third and the fifth flash in a row, in order to correct for acceptor side contributions at the same wavelength (for a detailed description of the correction and of the fit procedure, see Ref. [27]). The rapid, and here unresolved jump between the dashed lines represented absorption changes due to the transition $S_1 \Rightarrow S_2$. The subsequent slow decay was attributable to the electron transfer from the Mn-cluster to Y_Z. In Fig. 7A, it was fitted by a grey line. The half-decay times at temperatures of 3.9, 6, 12.1, and 20.6 °C, were 3.04, 2.76, 2.05 and 1.35 ms, respectively. The Arrhenius parameters of the UV-transients (slow phase) were as follows, $E_a = 33$ (± 1) kJ/mol, and $\ln A = 12.8$ (± 0.2). These rise times were of the same order of magnitude but slightly longer than those found at each temperature by oxygen polarography (see Section 4). Again, the Arrhenius plot was linear (see Fig. 6, open circles), so that the analysis of UV-transients gave no evidence for a temperature-dependent switching from one particular to another rate-limiting reaction.

We asked whether a similar lag-phase as evident from the polarographic measurements of oxygen evolution was also present in the UV absorption transients. And if not, had it perhaps escaped detection? A superimposition of a polarographic transient at 5.5 °C and a UV absorption transient at 6 °C revealed that a lag-phase of similar extent was absent in the UV measurement during the $S_3 \Rightarrow S_0$ transition. Such a lag-phase would have been discernible at the given noise level of the UV signal. The black bar in Fig. 7B points up the duration of the lag-phase of the polarographic transient. Apparently there was no lag phase of the electron transfer from the Mn-cluster to Y_Z. It corroborated the previous attribution of the lag to the liberation of formed oxygen from the catalyst into the medium.

3.4. Comparison between different starting materials and of UV spectroscopy versus polarography

The first two rows in Table 1 show the half-rise times that were obtained in the same material, *Synechocystis*, when detecting dioxygen polarographically and electron transfer by UV flash photometry. At four temperatures ranging from 3.9 to 20.6 °C, the half-rise times were of similar magnitude at any temperature. The polarographically determined times were shorter rather than longer than the UV-detected ones (see Section 4). Because oxygen evolution was the second-

Table 1
Comparison of the temperature-dependent half-rise times (in ms) of the S-state transition $S_3 \Rightarrow S_0$ from polarographic[a] and spectroscopic measurements

Material/method	Temperature (°C)			
	3.9	6	12.1	20.6
Synechocystis core complexes/UV spectroscopy	3.0	2.8	2.1	1.4
Synechocystis membranes/polarography[a]	2.9	2.5	1.8	1.1
Spinach BBY polarography[a]	4.5	4.0	3.2	2.1

[a] Data as determined from the line of best fit.

ary event following the reduction of Y_Z by the Mn-cluster, almost equal half-rise times proved that the polarographic signal was not diffusion-limited but presented the true rate of oxygen production. The two lower rows in Table 1 show the comparison between half-rise times of polarographic transients obtained with *Synechocystis* and with *Spinacia* membranes.

4. Discussion

PSII produces dioxygen in a four-stepped redox process. The primary substrate, water, is rapidly exchangeable even when the catalytic Mn-cluster has reached its penultimate oxidation state, S_3 [10–13]. Oxygen is only liberated when the Mn-cluster resides in its third oxidation state and after the redox active tyrosine, Y_Z, is oxidised again. We found that the rate of dioxygen release—it was measured polarographically with a centrifuged Pt-electrode over a wide temperature range—about equalled the rate of the electron transfer between the Mn-cluster and Y_Z^{ox}, as detected by flash photometry in the UV (see Table 1). Slight differences between these rates were attributable to different starting materials used in these two types of experiments (see Section 3). The broad coincidence between the rates had two aspects: (i) it proved the kinetic competence of the centrifugatable electrode, which was all but trivial, and (ii) it pointed, much to our regret, to the absence of sizable intermediates of the final catalytic step of oxygen production.

4.1. On the kinetic competence for photosynthetic oxygen evolution of the centrifugatable, bare Pt-electrode

A theory for the diffusion-limited oxygen supply from a layer of PSII membranes to a Pt-electrode has been developed by Lavorel [43]. Under certain idealising assumptions—a very rapid and stepped oxygen production by a single very thin layer at distance X from the electrode surface—this theory has yielded (i) a short lag phase, followed by (ii) the diffusion controlled rise of the amperometric signal up to (iii) a maximum, and (iv) the slower decay of this signal reflecting oxygen consumption by the electrode. Under these idealisations the characteristic (lag-, half-rise, peak-, half-decay) times were in strict proportion and related to each other as (i)/(ii)/(iii)/(iv) = 0.218/0.436/1/3.14 [43]. Lavorel has found these proportions and validated his theory by experiments, where he deposited one oxygen-evolving layer of membranes on a variable number of several heat-inactivated ones which merely served as spacers. The same proportions, however, were not at all met by our data, and it was obvious that the theory and its simplifications did not apply to our experimental situation. Instead, there were several lines of data, showing that it did not.

- The electron transfer from the Mn-cluster to Y_Z is the precursor of oxygen release. The slightly shorter rise of the polarographic transient (in PSII membranes) in comparison with the rise of its precursor, the UV-transient (in PSII core particles), proved that the oxygen electrode was kinetically competent.
- At 20 °C the observed rise time was 1.1 ms (*Synechocystis* membranes), and the (temperature-independent) electrode-plus-amplifier rise time was 100 μs (see Section 2). As a consequence, the instrument itself was not rate-limiting.
- Centrifugation of different amounts of PSII membranes on the Pt-electrode did neither affect the time lag nor the rise of the polarographic transient, but only its decay. Oxygen-evolving centres located directly on the platinum surface were apparently ‘‘seen’’ by the electrode with almost no influence of diffusion. Oxygen emerging from centres that were farther away from the platinum-surface or sticking to inactive patches on the platinum surface had longer diffusion path. These centres increased the source strength of the sample and thereby retarded the decay of the polarographic-signal (see Fig. 3).
- We characterised two mutants with about tenfold longer electron transfer time into and between Mn and Y_Z (UV-transient) and likewise tenfold longer rise-time of oxygen evolution (polarography), as detected by the same electrode (data for mutant D1–D61A not shown).

These data showed that the electrode response was not limited by the diffusion of oxygen to the metal surface.

4.2. The rise time of oxygen evolution and its temperature dependence

At a temperature of about 20 °C we found a half-rise time of oxygen evolution of about 1 ms with slight variation between PSII membranes and solubilised core preparations and between species. Our data (see Table 2) were in the range of data from the literature that were obtained by

Table 2
Half-rise times from polarographic measurements with cells or membranes

Material	Half-rise time (ms)	Temperature (°C)
Synechocystis cells	measured, 2.7[a,b] intrinsic, 1.2	ca. 20
Synechocystis cells	measured, 3 intrinsic, ≈ 1.5[c]	ca. 20
Synechocystis membranes	1.07[d]	20.6
Synechocystis membranes	1.3[e,f]	not specified
Spinach BBY	2.12[d]	20.6
Pea thylakoids	1.6[g]	20

[a] From Ref. [24].
[b] From Ref. [56].
[c] From Ref. [25].
[d] This work.
[e] From Ref. [22].
[f] From Ref. [23].
[g] From Ref. [17].

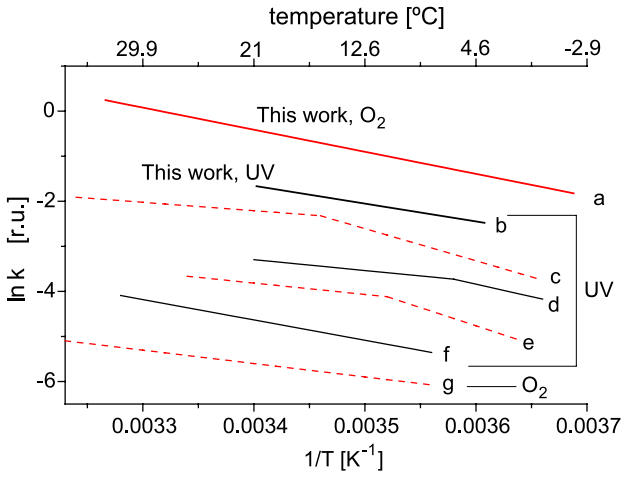

Fig. 8. Comparison of Arrhenius plots of the transition $S_3 \Rightarrow S_4 \rightarrow S_0$ (literature data and this work). For better visual comparison the preexponential factor, (a) was arbitrarily shifted. Spectroscopic transients that were reported by some authors revealed a breakpoint of the Arrhenius plots (c, d, e); however, the break-temperatures differed from each other, e.g. 6 °C (d), 11 °C (e) and 16 °C (c). Two sets of polarographic measurements (including those reported herein) did not exhibit a breakpoint (a and g), just like some UV data (line b, f). Data from a, b, this work; c, Ref. [31]; d, Ref. [39]; e, Ref. [40]; f, Ref. [17]; g, Ref. [42] (For color see online version).

centrifugatable oxygen electrodes (see Table 2 and Fig. 6 and references in the legend). We attributed variations of the respective half-rise times and of the activation energies to different starting materials (membranes versus core particles—bacteria versus plants) rather than primarily to different instrumentation. This is in line with results from Refs. [36,37], where it has been shown that detergent solubilization slows down the $S_3 \Rightarrow S_4 \rightarrow S_0$ transition (Fig. 8). This was also evident from polarographic data obtained with the same instrument and different material (Table 1). That the polarographic transient rose more rapidly than the UV transient, the latter indicative of electron transfer from the Mn-cluster and being the cause of oxygen production, left no doubt as to the kinetic competence of the electrode. We found no deviation from a linear Arrhenius plot of oxygen evolution in the temperature range from −2 and +32 °C. Likewise, we found no deviation from a linear Arrhenius plot of the UV-transients. Thus there was no evidence for a sequential reaction with a sizable intermediate of oxygen production, based on this approach.

Our results confirmed old polarographic data from literature, which were measured without a centrifugatable and highly time-resolving electrode and also yielded a continuous activation energy without any kink in the measured temperature region (Table 3). Sinclair and Arnason [42] have studied cells of the green algae *Chlorella vulgaris* and *C. pyrenoidosa* between 8 and 42 °C and determined an E_a of 24.7 kJ/mol.

4.3. The time lag of oxygen evolution as evidence for a short-lived intermediate

In contrast to previous studies, we corrected for artefacts of the polarographic method, namely direct photoelectric effects of the electrode itself and electrosmog. This allowed to detect a rather short, temperature-dependent lag phase of oxygen evolution (duration ≈ 450 μs at 20 °C) both in the WT and likewise in mutants with tenfold longer rise time of oxygen liberation (up to 13 ms). This lag phase was independent of the amount of material that was spun down on the electrode, and it was absent in UV-transients (see Fig.

Table 3
Activation energy of the transition $S_3 \Rightarrow S_0$ in dependence of material, preparation and method

Material (organism and preparation)	Discontinuity	Activation energy "spectroscopy" in kJ/mol	Activation energy "polarography" in kJ/mol	Range of temperature (°C)
Cells of *C. pyrenidosa*	no		32.2[a]	3 and 27
Cells of *C. pyrenidosa*	no		27.6[b]	9 and 26
Cells of *C. pyrenidosa* and *C. vulgaris*	no		24.7[c]	8–42
Spinach BBY	no		29.8 ± 0.8[d]	0.82–30.8
Synechocystis membranes	no		40.75 ± 0.9[d]	−2.1 to 31.7
Synechocystis-core complexes	no	33 ± 1[d]		3.9, 6, 12.1 and 20.6
Pea core complexes	no	37.5 ± 2[e]		7.9–30.6
Core complexes of *S. vulcanus*	yes	15.5 (T>16 °C)[f] 59.4 (T<16 °C)		1–50
Spinach core complexes	yes	21 (T>11 °C)[g] 67 (T<11 °C)		2–25
Spinach BBY	yes	20 (T>6 °C)[h] 46 (T<6 °C)		0.3–21

[a] From Ref. [57].
[b] From Ref. [58].
[c] From Ref. [42].
[d] This work.
[e] From Ref. [17].
[f] From Ref. [31].
[g] From Ref. [40].
[h] From Ref. [39].

7). The duration of the lag-phase increased with lower temperatures (see Fig. 5 and Section 3.1). Although both the half-rise time of oxygen evolution and the half-rise time of the reduction of Y_Z were retarded in parallel about tenfold in the mutant in comparison to the WT*, the same lag-phase of the oxygen transient occurred in both, whereas being absent in the UV-transients. Accordingly, this lag was attributable to the formation and/or liberation of oxygen proper and not to the electron transfer from bound water to the Mn-cluster and further on to Y_Z. In a sense, it was attributable to an intermediate with the same oxidation state as dioxygen and appearing only when the Mn-cluster was in its lowest oxidation state, S_0. Whether this intermediate was of chemical interest or trivial (freshly formed but still bound oxygen) remained to be established.

Acknowledgements

We thank Hella Kenneweg and Gabriele Hikade for excellent technical assistance and Dr. R. Ahlbrink and Prof. H.W. Trissl for discussions and help with the deconvolution algorithm. Financial support: Deutsche Forschungsgemeinschaft (SFB431-D8 and Ju97/15-1), Fonds der Chemischen Industrie, Land Niedersachsen (all to WJ) and NSF MCB-0111065 (to RD).

References

[1] R.D. Britt, Oxygenic photosynthesis: the light reactions, in: D. Ort, C.F. Yocum (Eds.), Oxygen Evolution, Kluwer Academic Publishing, Dordrecht, 1996, pp. 137–164.
[2] V.K. Yachandra, K. Sauer, M.P. Klein, Manganese cluster in photosynthesis: where plants oxidize water to dioxygen, Chem. Rev. 96 (1996) 2927–2950.
[3] J.E. Penner-Hahn, Structure and bonding, Structural Characterization of the Mn Site in the Photosynthetic Oxygen-Evolving Complex, Springer-Verlag, Heidelberg, 1998, pp. 1–36.
[4] C.W. Hoganson, G.T. Babcock, Mechanistic aspects of the tyrosyl radical–manganese complex in photosynthetic water oxidation, Met. Ions Biol. Syst. 37 (2000) 613–656.
[5] R.J. Debus, The polypeptides of photosystem II and their influence on maganotyrosyl-based oxygen evolution, Met. Ions Biol. Syst., (2000) 657–711.
[6] V.L. Pecoraro, W.Y. Hsieh, The use of model complexes to elucidate the structure and function of manganese redox enzymes, Met. Ions Biol. Syst. 37 (2000) 429–504.
[7] C. Tommos, G.T. Babcock, Proton and hydrogen currents in photosynthetic water oxidation, Biochim. Biophys. Acta 1458 (2000) 199–219.
[8] G. Renger, Photosynthetic water oxidation to molecular oxygen: apparatus and mechanism, Biochim. Biophys. Acta 1503 (2001) 210–228.
[9] J. Messinger, J.H. Robblee, U. Bergmann, C. Fernandez, P. Glatzel, H. Visser, R.M. Cinco, K.L. McFarlane, E. Bellacchio, S.A. Pizarro, S.P. Cramer, K. Sauer, M.P. Klein, V.K. Yachandra, Absence of Mn-centered oxidation in the S-2 → S-3 transition: implications for the mechanism of photosynthetic water oxidation, J. Am. Chem. Soc. 123 (2001) 7804–7820.
[10] J. Messinger, M. Badger, T. Wydrzynski, Detection of *one* slowly exchanging substrate water molecule in the S3 state of photosystem II, Proc. Natl. Acad. Sci. U. S. A. 92 (1995) 3209–3213.
[11] W. Hillier, J. Messinger, T. Wydrzynski, Kinetic determination of the fast exchanging substrate water molecule in the S_3 state of photosystem II, Biochemistry 37 (1998) 16908–16914.
[12] W. Hillier, G. Hendry, R.L. Burnap, T. Wydrzynski, Substrate water exchange in photosystem II depends on the peripheral proteins, J. Biol. Chem. 276 (2001) 46917–46924.
[13] G. Hendry, T. Wydrzynski, The two substrate-water molecules are already bound to the oxygen-evolving complex in the S2 state of photosystem II, Biochemistry 41 (2002) 13328–13334.
[14] G. Renger, T. Bittner, J. Messinger, Structure–function relationships in photosynthetic water oxidation, Biochem. Soc. Trans. 22 (1994) 318–322.
[15] F. Rappaport, M. Blanchard-Desce, J. Lavergne, Kinetics of electron transfer and electrochromic change during the redox transition of the photosynthetic oxygen-evolving complex, Biochim. Biophys. Acta 1184 (1994) 178–192.
[16] G. Renger, Photosynthetic oxygen evolution, in: H. Metzner (Ed.), Theoretical Studies About the Functional and Structural Organization of the Photosynthetic Oxygen Evolution, Academic Press, London, 1978, pp. 229–248.
[17] M. Haumann, O. Bögershausen, D.A. Cherepanov, R. Ahlbrink, W. Junge, Photosynthetic oxygen evolution: H/D isotope effects and the coupling between electron and proton transfer during the redox reactions at the oxidizing side of photosystem II, Photosynth. Res. 51 (1997) 193–208.
[18] M. Haumann, W. Junge, Photosynthetic water oxidation: a simplex-scheme of its partial reactions, Biochim. Biophys. Acta 1411 (1999) 86–91.
[19] N. Kamiya, J.R. Shen, Crystal structure of oxygen-evolving photosystem II from *Thermosynechococcus vulcanus* at 3.7-angstrom resolution, Proc. Natl. Acad. Sci. U. S. A. 100 2003, pp. 98–103.
[20] A. Zouni, H.T. Witt, J. Kern, P. Fromme, N. Krauss, W. Saenger, P. Orth, Crystal structure of photosystem II from *Synechococcus elongatus* at 3.8 Å resolution, Nature 409 (2001) 739–743.
[21] S. Vasil'ev, P. Orth, A. Zouni, T.G. Owens, D. Bruce, Excited-state dynamics in photosystem II: insights from the X-ray crystal structure, Proc. Natl. Acad. Sci. U. S. A. 98 2001, pp. 8602–8607.
[22] M. Qian, L. Dao, R.J. Debus, R.L. Burnap, Impact of mutations within the putative Ca^{2+}-binding lumenal interhelical a–b loop of the photosystem II D1 protein on the kinetics of photoactivation and H_2O-oxidation in *Synechocystis* sp. PCC6803, Biochemistry 38 (1999) 6070–6081.
[23] Z.L. Li, R.L. Burnap, Mutations of arginine 64 within the putative Ca^{2+}-binding lumenal interhelical a–b loop of the photosystem II D1 protein disrupt binding of the manganese stabilizing protein and cytochrome *c*(550) in *Synechocystis* sp. PCC6803, Biochemistry 40 (2001) 10350–10359.
[24] M. Hundelt, A.M. Hays, R.J. Debus, W. Junge, Oxygenic photosystem II: the mutation D1–D61N in *Synechocystis* sp. PCC 6803 retards S-state transitions without affecting electron transfer from Y_Z to P_{680}^+, Biochemistry 37 (1998) 14450–14456.
[25] M. Hundelt, A.M.A. Hays, R.J. Debus, W. Junge, The mutation D1–D61N in PSII of *Synechocystis*: retardation of ET from OEC → Y_Z^{ox} and no effect on $Y_Z \rightarrow P_{680}^+$, in: G. Garab (Ed.), Photosynthesis: Mechanisms and Effects, vol. 2. Kluwer Academic Publishing, Dordrecht, 1998, pp. 1387–1390.
[26] J. Clausen, S. Winkler, A.M.A. Hays, M. Hundelt, R.J. Debus, W. Junge, PS2001 Proceedings—12th International Congress on Photosynthesis, Mutations D1-E189K, R and Q of *Synechocystis* sp. PCC6803 Are Without Influence on Ns-to-Ms Electron Transfer Between OEC-Y_Z-P_{680} in Photosystem II, Csiro Publishing, Collingwood, Vic. 3066, Australia, 2001, pp. 1–5.
[27] J. Clausen, S. Winkler, A.M.A. Hays, M. Hundelt, R.J. Debus, W. Junge, Photosynthetic water oxidation: mutations of D1-Glu189K, R and Q of *Synechocystis* sp. PCC6803 are without any influence on electron transfer rates at the donor side of photosystem II, Biochim. Biophys. Acta 1506 (2001) 224–235.

[28] J.P. Dekker, J.J. Plijter, L. Ouwehand, H.J. van Gorkom, Kinetics of manganese redox transitions in the oxygen evolving apparatus of photosynthesis, Biochim. Biophys. Acta 767 (1984) 176–179.
[29] J.P. Dekker, D.F. Ghanotakis, J.J. Plijter, H.J. van Gorkom, G.T. Babcock, Kinetics of the oxygen-evolving complex in salt-washed photosystem II preparations, Biochim. Biophys. Acta 767 (1984) 515–523.
[30] G. Renger, W. Weiss, Studies on the nature of the water oxidizing enzyme: III. Spectral characterization of the intermediary redox states in the water-oxidizing enzyme system Y, Biochim. Biophys. Acta 850 (1986) 184–196.
[31] H. Koike, B. Hanssum, Y. Inoue, G. Renger, Temperature dependence of S-state transition in a thermophilic cyanobacterium, *Synechococcus vulcanus* Copeland measured by absorption changes in the ultraviolet region, Biochim. Biophys. Acta 893 (1987) 524–533.
[32] M. Haumann, M. Hundelt, P. Jahns, S. Chroni, O. Bögershausen, D. Ghanotakis, W. Junge, Proton release from water oxidation by photosystem II: similar stoichiometries are stabilized in thylakoids and core particles by glycerol, FEBS Lett. 410 (1997) 243–248.
[33] Ö. Saygin, H.T. Witt, Optical characterization of intermediates in the water-splitting enzyme system of photosynthesis—possible states and configurations of manganese and water, Biochim. Biophys. Acta 893 (1987) 452–469.
[34] G.T. Babcock, R.E. Blankenship, K. Sauer, Reaction kinetics for positive charge accumulation on the water side of chloroplast photosystem II, FEBS Lett. 61 (1976) 286–289.
[35] K. Strzalka, T. Walczak, T. Sarna, H.M. Swartz, Measurement of time-resolved oxygen concentration changes in photosynthetic systems by nitroxide-based EPR oximetry, Arch. Biochem. Biophys. 281 (1990) 312–318.
[36] M.R. Razeghifard, C. Klughammer, R.J. Pace, Electron paramagnetic resonance kinetic studies of the S states in spinach thylakoids, Biochemistry 36 (1997) 86–92.
[37] M.R. Razeghifard, R.J. Pace, EPR kinetic studies of oxygen release in thylakoids and PSII membranes: an intermediate in the S_3 to S_0 transition, Biochemistry 38 (1999) 1252–1257.
[38] M. Haumann, W. Junge, Extent and rate of proton release by photosynthetic water oxidation in thylakoids: electrostatic relaxation versus chemical production, Biochemistry 33 (1994) 864–872.
[39] G. Renger, B. Hanssum, Studies on the reaction coordinates of the water oxidase in PS II membrane fragments from spinach, FEBS Lett. 299 (1992) 28–32.
[40] M. Karge, K.D. Irrgang, G. Renger, Analysis of the reaction coordinate of photosynthetic water oxidation by kinetic measurements of 355 nm absorption changes at different temperatures in photosystem II preparations suspended in either H_2O or D_2O, Biochemistry 36 (1997) 8904–8913.
[41] G. Renger, Mechanistic and structural aspects of photosynthetic water oxidation, Physiol. Plant. 100 (1997) 828–841.
[42] J. Sinclair, T. Arnason, Studies on a thermal reaction associated with photosynthetic oxygen evolution, Biochim. Biophys. Acta 368 (1974) 393–400.
[43] J. Lavorel, Determination of the photosynthetic oxygen release time by amperometry, Biochim. Biophys. Acta 1101 (1992) 33–40.
[44] A.M. Hays, I.R. Vassiliev, J.H. Golbeck, R.J. Debus, Role of D1-His190 in the proton-coupled oxidation of tyrosine Y_Z in manganese-depleted photosystem II, Biochemistry 38 (1999) 11851–11865.
[45] H.A. Chu, A.P. Nguyen, R.J. Debus, Site-directed photosystem II mutants with perturbed oxygen-evolving properties. 1. Instability or inefficient assembly of the manganese cluster in vivo, Biochemistry 33 (1994) 6137–6149.
[46] H.A. Chu, A.P. Nguyen, R.J. Debus, in: P. Mathis (Ed.), Photosynthesis: from Light to Biosphere, An Improved Host Strain of *Synechocystis* sp. PCC 6803 for Introducing Site-Directed Mutations into the D1 Protein of Photosystem II, vol. 2, Kluwer Academic Publishing, Dordrecht, 1995, pp. 439–442.
[47] H.K. Lichtenthaler, Chlorophylls and carotenoids: pigments of photosynthetic biomembranes, Methods Enzymol. 148 (1987) 350–382.
[48] R. Burnap, H. Koike, G. Sotiropoulou, L.A. Sherman, Y. Inoue, Oxygen evolving membranes and particles from the transformable cyanobacterium *Synechocystis* sp. PCC6803, Photosynth. Res. 22 (1989) 123–130.
[49] D.A. Berthold, G.T. Babcock, C.F. Yocum, A highly resolved, oxygen-evolving photosystem II preparation from spinach thylakoid membranes, FEBS Lett. 134 (2) 231–234.
[50] P.J. van Leeuwen, M.C. Nieveen, E.J. van de Meent, J.P. Dekker, H.J. van Gorkom, Rapid and simple isolation of pure photosystem II core and reaction center particles from spinach, Photosynth. Res. 28 (1991) 149–153.
[51] B. Forbush, B. Kok, M.P. McGloin, Cooperation of charges in photosynthetic O_2 evolution: II. Damping of flash yield oscillation, deactivation, Photochem. Photobiol. 14 (1971) 307–321.
[52] W. Junge, in: T.W. Goodwin (Ed.), Chemistry and Biochemistry of Plant Pigments, Flash Kinetic Spectrophotometry in the Study of Plant Pigments, Academic Press, London, 1976, pp. 233–333.
[53] O. Bögershausen, W. Junge, Rapid proton transfer under flashing light at both functional sides of dark adapted photosystem II core particles, Biochim. Biophys. Acta 1230 (1995) 177–185.
[54] H.J. van Gorkom, P. Gast, in: J. Amesz, A.J. Hoff (Eds.), Biophysical Techniques in Photosynthesis,3, Measurement of Photosynthetic Oxygen Evolution, Kluwer Academic Publishing, Dordrecht, 1996, pp. 391–405.
[55] R.C. Weast, M.J. Astle, CRC Handbook of Chemistry and Physics, CRC Press, Boca Raton, USA, 1979.
[56] M. Hundelt, Photosynthetische Wasseroxidation in PSII: Elektronen Und Protonentransfer Im Wildtyp Und in D1-Mutanten Von *Synechocystis* sp. PCC 6803, Universität Osnabrück, Osnabrück, 1999.
[57] P. Joliot, M. Hofnung, R. Chabaud, Etude de l'emission d'oxygene par des algues soumises a un eclairement module sinusoidalement, J. Chim. Phys. 63 (1966) 1423–1441.
[58] A.L. Etienne, Etude de l'etape thermique de l'emission photosynthetique d'oxygene par une methode d'ecoulement, Biochim. Biophys. Acta 153 (1968) 895–897.
[59] M.R. Razeghifard, R.J. Pace, Electron paramagnetic resonance kinetic studies of the S states in spinach PSII membranes, Biochim. Biophys. Acta 1322 (1997) 141–150.
[60] C.W. Hoganson, G.T. Babcock, Electron-transfer events near the reaction center in O_2-evolving photosystem II preparations, Biochemistry 27 (1988) 5848–5855.